Cellular Broadband Millimeter Wave Propagation and Angle of Arrival for Adaptive Beam Steering Systems (Invited Paper)

Theodore S. Rappaport, Yijun Qiao, Jonathan I. Tamir, James N. Murdock, Eshar Ben-Dor

Wireless Networking and Communications Group (WNCG)
Electrical and Computer Engineering Department, The University of Texas at Austin, Austin, TX 78712
wireless@mail.utexas.edu

***Abstract* — The advent of inexpensive millimeter wave devices and steerable antennas will lead to future cellular networks that use carrier frequencies at 28 GHz, 38 GHz, 60 GHz, and above. At these frequencies, the available RF bandwidth is much greater than that of current 4G systems, and high gain millimeter wave steerable antennas can be made in much smaller form factor than current products. This paper presents an extensive measurement campaign and initial results for base-station - to - mobile propagation situations at 38 GHz carrier frequencies in an outdoor urban environment using directional, steerable antennas. This work provides angle of arrival (AOA) and RF multipath characteristics for highly directional antenna beams that may exploit non-line-of-sight propagation paths for futuristic channels at 38 GHz. This work yields data for a variety of antenna pointing and antenna beamwidth scenarios in line-of-sight (LOS) and non-line-of-sight (NLOS) scenarios.**

***Index Terms* — millimeter wave, AOA, 38 GHz propagation measurements, cellular, mobile communication system.**

I. INTRODUCTION

The proliferation of wireless services and technologies has resulted in a global bandwidth shortage, as wireless carrier-frequencies have been range-bound from 800 MHz to 5.8 GHz [1]. There is growing interest in the use of wireless millimeter-wave (i.e. carrier frequency > 30 GHz) frequencies, where available bandwidth exceeds the combined bandwidths of all wireless communication systems in widespread use today [1].

Some of the earliest uses of millimeter-wave frequencies were LMDS (Local Multipoint Distribution System) and Backhaul services at 20 and 40 GHz in the 1990s, but these were commercially unsuccessful due to high hardware costs associated with millimeter-wave devices. Advancements in CMOS production technologies, however, have led to great cost and size reductions of these devices, making millimeter-wave frequencies an attractive and now cost-effective means of alleviating the bandwidth crisis. Devices such as smart antenna arrays and low power wide spectrum millimeter wave circuits may soon become prevalent as industry leaders look to millimeter-wave frequencies as a means to continue wireless technological development in the coming decades [2],[3].

Understanding radio channel propagation characteristics at these millimeter wave frequencies is crucial for the design of future communication systems [4],[5]. In [6], the 60 GHz peer-to-peer channel was measured for an outdoor urban setting to enable *ad hoc* millimeter wave communication systems with high-directionality antennas. In [7], 38GHz measurements were compared with 60 GHz peer-to-peer channels, and 38GHz rooftop-to-ground (cellular) measurements were presented. A 38 GHz outdoor cellular outage study using highly directional, steerable antennas with two different transmitter base station antenna heights was studied in [8].

Several others have measured the outdoor propagation environment at millimeter wave frequencies focusing on LMDS applications, which involve elevated, stationary antennas. In [9], [10], and [11], channels were measured during regular, rain, and hail conditions at various ranges and frequencies. [12] and [13] noted that propagation obstacles, including tree canopies and rooftops, can limit throughput at millimeter wave frequencies, and contended that line-of-sight (LOS) paths may be the only viable means for sufficient signal strength. None of the previous studies examined the millimeter wave outdoor channel for cellular applications. However, [8] demonstrated that non-LOS (NLOS) paths may be used reliably if cell sizes are kept to approximately 200 m in radius.

In this paper, we present 38 GHz rooftop-to-ground (or "cellular") angle-of-arrival channel measurements taken at The University of Texas at Austin. We collected over 700 measurements at 37 unique receiver locations and four unique transmitter base station locations, chosen to represent typical urban cellular channels with varying base station heights. Our measurement system used an EIRP of 46.2 dBm, and was capable of measuring path loss up to 158 dB using highly directional and steerable antennas. Power delay profiles (PDPs) were captured using a sliding correlator channel sounder to fully characterize the channel. Two different horn receiver antennas with gains of 13.3 and 25 dBi were used to test the impact of antenna beamwidth on received signal strength and RMS (Root-mean-Square) delay spread. Notably, measurements using the 13.3 dBi receiver antenna showed less path loss in obstructed LOS conditions and RMS delay spreads nearly equivalent to the spreads measured with the 25 dBi receiving antenna. In addition to computing path loss and RMS delay spread, we recorded the TR separation distances, and azimuth and elevation angles for both the transmitter and receiver antennas for each measurement. These additional parameters afford in-depth analysis of the trade-offs between receiver antenna type, steering angle, and propagation distance in relation to path loss and RMS delay spread. We also define a new parameter, the *arc length*, to encapsulate the impact of antenna pointing angles and transmitter-receiver separation distance into a single parameter.

This paper is organized as follows: Section II describes the channel measurement system and outlines the experiment design and the measurement process; Section III presents the

measurement results. Finally, Section IV provides a conclusion to the paper.

II. Measurement Procedure

A 400Mcps sliding correlator channel sounder [14] was used for the cellular measurements. The baseband spread spectrum signal was upconverted to 37.625GHz and transmitted through a 7.8° beamwidth Ka-band vertically polarized 25 dBi horn antenna with 21.2 dBm applied to the antenna input. Two interchangeable antennas were used at the receiver. The first was a 7.8° beamwidth Ka-band vertically polarized 25 dBi horn antenna, and the second was a 49° beamwidth Ka-band vertically polarized 13.3 dBi horn antenna. The system used a slide factor of 8000 to provide a temporal resolution of 2.33 ns and 158 dB of path loss sensitivity.

The transmitter was placed at four locations within The University of Texas at Austin campus. At each location, the transmitter antenna was mounted on a tripod 1.5 m above the roof toward the building's edge. The first two transmitter locations were along the northern and eastern edges of the rooftop of an eight-story building (36 m). The third location was on the northern edge of a five-story rooftop (23 m). The last transmitter location was closer to the ground, at approximately 8 meters above a recessed parking lot and busy four lane avenue. For each transmitter location, about eleven receiver positions were chosen for measurements with the 25 dBi receiver antenna, and about five of the locations for each transmitter position were revisited and measured with the 13.3 dBi receiver antenna. The receiver locations represented typical outdoor urban cellular environments, in which a user may have clear LOS to the transmitter, partially obstructed LOS due to foliage, or NLOS due to buildings or other large obstructions. The 25 dBi receiver antenna locations ranged from 29 m to 930 m from the transmitter. The 13.3 dBi antenna locations were between 70 m and 728 m from the transmitter.

Highly directional antennas at the transmitter and receiver enabled scanning in both azimuth and elevation angular directions to establish links, similar to a steerable antenna array. At each receiver location, measurements were conducted for one to fourteen unique transmitter-receiver antenna angle combinations that resulted in links. For the LOS and partially obstructed LOS links, the transmitter and receiver antennas were pointed toward each other. The NLOS links were found using a manual steering approach. First, the transmitter antenna was steered toward a potential scatterer, such as a lamppost, building, tree, or automobile. Next, the receiver antenna was steered along its azimuth and elevation planes to search for a signal. At each location, each measurement at that location was formed by spatial averaging PDPs from eight local positions at the measurement location equally spaced by 10 λ (8 cm) along a circular track. At each position on the track, the receiver antenna was slightly reoriented to point toward the supposed cause of the received signal (e.g. to a reflecting building or lamppost). Each acquired PDP for each local position on the circular track was the result of averaging 20 PDPs acquired by software in rapid succession over a few seconds. After the spatial averaging of the local position PDPs, the average PDP was manually thresholded at the noise floor to distinguish between channel-induced multipath and noise when computing channel statistical parameters.

III. Results and Analysis

The excess path loss and RMS delay spread were computed for all 731 measurements recorded in the campaign. Excess path loss was calculated with respect to a five meter free space reference. The path-loss exponents for the clear LOS, partially obstructed LOS, and NLOS measurements were separately computed to compare the characteristics of obstructed and NLOS paths to the characteristics of clear LOS links for which no clutter or vegetation existed between the transmitter and receiver.

Fig. 1 shows a scatter plot of the path loss above 5 m free space reference (i.e. relative path loss) for each measurement acquired using the 25 dBi receiver antenna. The clear (i.e. no clutter or vegetation between the transmitter and receiver) LOS path loss exponent is 1.89, slightly below that of free space, and increases to 2.30 when partially obstructed LOS links are also considered. In contrast, the NLOS measurements are weaker than LOS paths by 10 to 30 dB and have a path loss exponent of 3.86. If only the best NLOS links at each location are considered (to mimic the performance of an adaptive antenna array that searches for the best link available), the path loss exponent is reduced to 3.2.

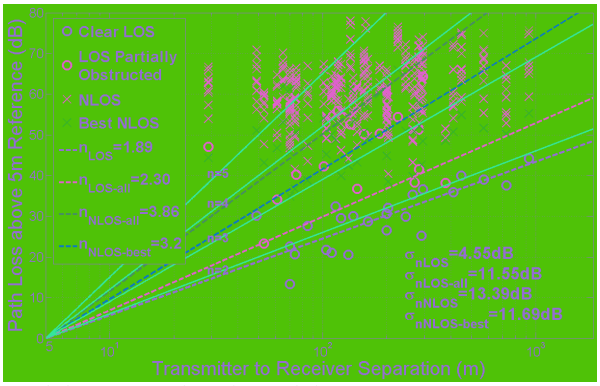

Fig. 1. Path loss scatter plot using 25dBi Rx antenna at 38 GHz. LOS and NLOS measurements have path loss exponents of 2.30 and 3.86, respectively, while the best NLOS links have a path loss exponent of 3.2.

Fig. 2 shows the path loss scatter plot for the measurements acquired using the wider beam 13.3 dBi receiver antenna. The path loss exponents for clear LOS and both clear and partially obstructed LOS are 1.90 and 2.21, respectively, while the exponent for NLOS measurements is 3.18. The best NLOS paths have an exponent of 2.56. Notably, the 13.3 dBi receiver antenna provides lower path-loss exponents for obstructed and NLOS links, in comparison to measurements obtained with the 25 dBi receiver antenna. The low NLOS path loss was caused by the remnant energy received from the LOS direction path due to the large beamwidth and fewer captured links above 60dB relative path loss due to the lower antenna gain. The path loss exponent observed for obstructed boresight direction links (i.e. partially obstructed LOS) was slightly lower due to the increase in scattering and diffracting paths which were captured by the receiver antenna.

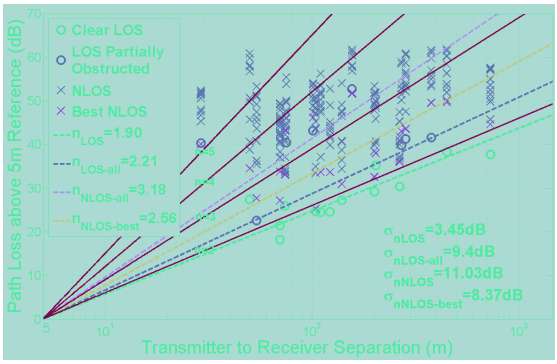

Fig. 2 Path loss scatter plot using 13.3 dBi RX antenna at 38GHz. Lower NLOS and partially obstructed LOS path loss exponents were observed due to increase in scattering and diffracting links captured by a wider beam antenna.

The CDFs of the RMS delay spreads for LOS and NLOS paths using each receiver antenna are shown in Fig. 3. The delay spreads with each antenna were nearly identical in distribution, despite the discrepancy in NLOS path loss. Most LOS measurements had the minimal RMS delay spread, on the order of 1.1 ns due to the pulse shape, with one partially obstructed LOS link resulting in a maximum of 15.5 ns. The NLOS measurements exhibited higher and more varied delay spreads, with a mean of 14.3 ns (for 25 dBi receiver antenna) and 13.7 ns (13.3 dBi receiver antenna). The maximum NLOS RMS delay spreads were 255 and 166 ns for 25 and 13.3 dBi receiver antennas, respectively. Nonetheless, more than 80% of the NLOS links had RMS delay spreads under 20 ns.

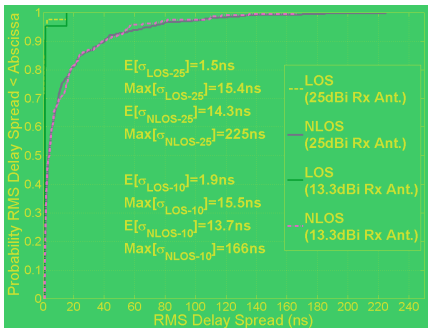

Fig. 3. RMS delay spread CDF for all 38GHz measurements. Measurements using 25dBi and 13.3dBi antennas show nearly identical delay spread CDFs.

RMS delay spread as a function of excess path loss (i.e. path loss in excess of the predicted free space loss) is shown in Fig. 4. As seen, weaker signals had probabilistically higher delay spreads, since multipath components become more prominent for weaker signals. However, the relationship between RMS delay spread and path loss was site-specific, as shown by the wide range of RMS delay spreads. For both antenna configurations, the RMS delay spread initially increases with excess loss and subsequently falls slowly. The peak RMS delay spreads occur at a lower excess loss for the 13.3 dBi antennas than the 25 dBi counterpart due to their lower gain. A low gain antenna is capable of capturing energy from more directions, yet fewer of the arriving multipath components are above the system sensitivity. Thus, the maximum RMS delay spread occurs at the best trade-off between antenna gain, which limits the number of multipath components above sensitivity level, and beamwidth, which determines the number of multipath components collected by the antenna.

RMS delay spreads for the 25 dBi and 13.3 dBi receiver antennas are plotted as a function of TR separation in Fig. 5. Generally, delay spread and TR separation are inversely proportional. As the separation increases, the signal strength decreases, thus multipaths drop below the minimal detectable signal level, lowering the RMS delay spread. This may play a role in future system design, as directional antennas can be used to maintain a low-interference link over large distances, yet less diversity can be exploited in a MIMO setting.

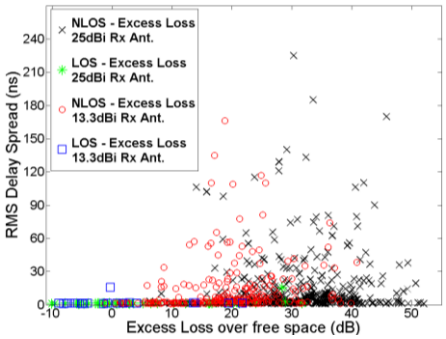

Fig. 4. RMS delay spread vs. excess path loss above free space predicted loss for 38GHz. Weak signals exhibit high delay spreads as weak multipath become important.

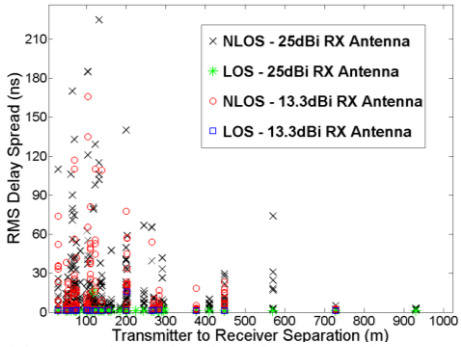

Fig. 5. RMS delay spread as a function of TR separation at 38GHz. Delay spread decreases over long paths since multipath drops below system sensitivity.

Fig. 6 shows the RMS delay spread as a function of combined antenna pointing angles, where the combined angle at each measurement is the sum of absolute transmitter and receiver azimuth angles off boresight plus the sum in elevation angle between the transmitter and receiver antennas. The elevation angle sum is zero when the antennas are pointing in the boresight direction (i.e. LOS). As expected, RMS delay spread increases with combined angle, as steeper angles are correlated with a higher number of signal bounces from the transmitter to the receiver. At small angles, both antennas exhibit low variance in delay spread.

As seen in Fig. 5 and Fig. 6, RMS delay spread is inversely proportional to TR separation distance and directly proportional to combined off-boresight angle. To study the importance of these two opposing trends, we introduce the *arc length* of a particular measurement, defined as the product of the TR separation and the combined off-boresight angle (in radians). Fig. 7 shows RMS delay spread vs. arc length over all measurements. As the plot shows, there is an inverse relationship on a large scale from 0 to 3000 m-rad. This decreasing trend matches that of Fig. 5, indicating that TR

separation distance is more important than off-boresight angle over large arc-lengths in determining RMS delay spread. However, a close-up of the plot for values below 300 m-rad suggests an opposite trend. In fact, at low arc lengths, the plot resembles Fig. 6, implying that the combined off-boresight angle is of higher importance. The transition point for this urban campus environment occurs at approximately 400 meter-radian, where distance begins dominating angle.

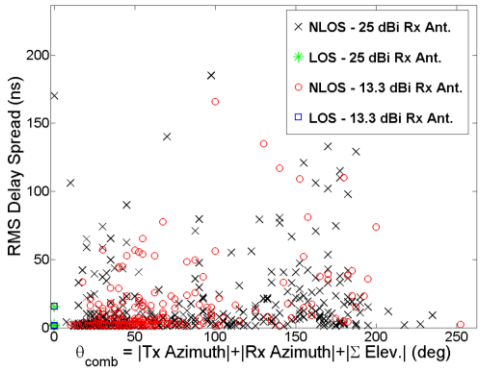

Fig. 6. RMS delay spread vs. off-boresight angle combination for 38GHz. The delay spread increases as the antennas point further away from boresight.

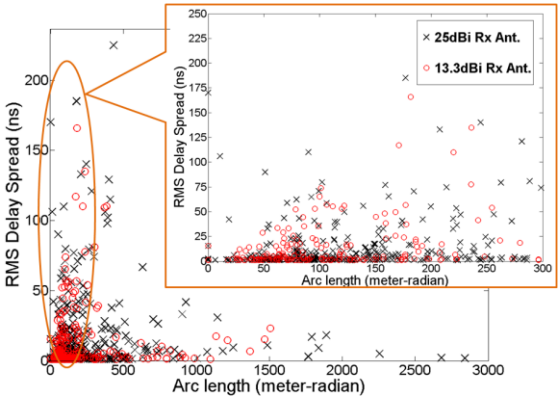

Fig. 7. RMS delay spread vs. arc length over all 38GHz measurements. The trend is decreasing, indicating that distance prevails over angle in determining delay spread. However, a close-up of low arc lengths shows the angle playing a larger role in determining delay spread.

IV. CONCLUSION

This work presented a study on 38 GHz propagation in an outdoor, urban, cellular environment. A summary of the path loss exponents and RMS delay spread distributions is provided in Table 1. Using highly directional, steerable antennas, a receiver is often able to establish as many as 14 links with a rooftop-mounted transmitter despite obstructions in the propagation path. The measured results, coupled with the outage study in [8], enable intelligent design of cellular base stations to fully exploit path diversity. We observed that a 13.3 dB horn antenna incurs less path loss than a 25 dBi horn antenna when pointing in NLOS directions or when the LOS direction is obstructed with foliage or other structures. The NLOS links have an average RMS delay spread of about 14 ns while minimal RMS delay spread was exhibited by the majority of LOS and partially obstructed LOS links. RMS delay spreads for both receiver antennas have similar CDFs, meaning the antenna beamwidth only marginally impacts the delay spread distribution. Additionally, observing the RMS delay spread as a function of the arc length (TR separation times combined angle) suggests that the RMS delay spread is a strong function of off-boresight angle for short links and dominated by TR separation for long links.

Table 1: Summary of path loss exponents and average and 99 percentile RMS delay spread for 38GHz results.

	25dBi RX Ant.		**13.3dBi RX Ant.**	
	LOS	NLOS	LOS	NLOS
Path Loss Exponent	2.30 (clear 1.89)	3.86 (best: 3.20)	2.21 (clear 1.90)	3.18 (best: 2.56)
Path Loss std. dev. (dB)	11.6 (clear 4.6)	13.4 (best 11.7)	9.4 (clear 3.5)	11.0 (best 8.4)
RMS Delay Spread (ns)	1.5 avg. 15.4 @99%	14.3 avg. 133 @99%	1.9 avg. 15.5 @ 99%	13.7 avg. 117 @ 99%

ACKNOWLEDGEMENT

This project is sponsored by Samsung Telecommunications America, LLC. The authors wish to thank Samuel J. Lauffenburger and Adrian Duran for their contributions. Work done under FCC Experimental License 0548-EX-PL-2010.

REFERENCES

[1] Rappaport, T.S., Murdock, J.N. Gutierrez, F., "State of the Art in 60 GHz Integrated Circuits and Systems for Wireless Communications," *Proceedings of the IEEE*, August, 2011, Vol. 99, no. 8, pp. 1390-1436.

[2] Velez, F.J., Dinis, M., Fernandes, J., "Mobile Broadband Systems: Research and Visions," *IEEE Vehicular Technology Society News*, Vol. 52, No. 2, pp. 4-12, May 2005.

[3] Murdock, J. N., Rappaport, T. S., "Consumption Factor: A Figure of Merit for Power Consumption and Energy Efficiency in Broadband Wireless Communication," *IEEE Globecom Conference 2011*, in press.

[4] Rajagopal, S., Abu-Surra, S., Pi, Z., Khan, F., "Antenna Array Design for Multi-Gbps mmWave Mobile Broadband Communication," *IEEE Globecom Conference 2011*, in press.

[5] Liberti, J.C., Rappaport, T.S., Smart Antennas for Wireless Communications: IS-95 and Third Generation CDMA Applications. Prentice Hall PTR, Upper Saddle River, NJ, USA, 1999.

[6] Ben-Dor, E., Rappaport, T.S., Qiao, Y., Lauffenburger, S.J., "Millimeter-wave Broadband Channel Sounder and Propagation Measurements for Wireless Communications," *IEEE Globecom Conference 2011*, in press.

[7] Rappaport, T.S., Ben-Dor, E., Murdock, J. N., Qiao, Y., "38 GHz and 60 GHz Angle-dependent Propagation for Cellular & Peer-to-Peer Wireless Communications," submitted to *IEEE ICC 2012*.

[8] Murdock, J.N., Ben-Dor, E., Qiao Y., Tamir, J.I., Rappaport, T.S., "A 38 GHz Cellular Outage Study for an Urban Outdoor Campus Environment," submitted to *IEEE WCNC 2012*.

[9] Xu, H., Rappaport, T.S., Boyle, R., Schaffner, J., "Measurements and Models for 38-GHz Point-to-Multipoint Radiowave Propagation," *IEEE Journal of Selected Areas in Communications*, Vol. 18, No. 3, Mar. 2000.

[10] Violette, E.J., Espeland, R.H., Hand,G.R., "Millimeter-Wave Urban and Suburban Propagation Measurements Using Narrow and Wide Bandwidth Channel Probes," NTIA Report 85-184, Nov. 1985.

[11] Zhao, Q., Jin, L., "Rain Attenuation in Millimeter Wave Ranges," *Int. Symp. On Antennas, Propagation & EM Theory*, pp. 26-29, Oct. 2006.

[12] Seidel, S.Y., Arnold, H.W., "Propagation measurements at 28 GHz to investigate the performance of local multipoint distribution service (LMDS)," IEEE Globecom Conference, Vol.1, pp.754-757, Nov. 1995.

[13] Papazian, P.B., Hufford, G.A., Achatz, R.J., Hoffman, R., "Study of the local multipoint distribution service radio channel," *IEEE Transactions on Broadcasting*, Vol.43, No.2, pp.175-184, June 1997.

[14] Rappaport, T.S., Wireless Communications, 2nd Ed, Prentice Hall, 2002.